Intensity coded octopaminergic modulation of aversive crawling behavior in *Drosophila melanogaster* larvae

Florian Bilz[1], Madeleine-Marie Gilles[1], Adriana Schatton[2], Hans-Joachim Pflüger[1, #] &

Marco Schubert[1, #]

[1] *Department of Biology, Chemistry and Pharmacy, Institute of Biology - Neurobiology, Freie Universität Berlin, Königin-Luise-Strasse 1-3, 14195 Berlin, Germany*

[2] *Department of Biology, Chemistry and Pharmacy, Institute of Biology - Animal Behavior, Freie Universität Berlin, Takustrasse 6, 14195 Berlin, Germany*

[#] *Shared senior authorship*

Correspondence: Dr. Marco Schubert,

Department of Biology, Chemistry and Pharmacy,

Institute of Biology – Neurobiology,

Freie Universität Berlin,

Königin-Luise-Strasse 1-3, 14195 Berlin, Germany.

Email: m.schubert@fu-berlin.de

Running title: bioaminergic modulation of crawling behavior

Abstract

35   Activation and modulation of sensory-guided behaviors by biogenic amines assure appropriate

36   adaptations to changes in an insect's environment. Given its genetic tool kit *Drosophila melanogaster*

37   represents an excellent model organism to study larger networks of neurons by optophysiological

38   methods. Here, we studied stationary crawling movements of 3rd instar larvae and revealed how the

39   octopaminergic VUM neuron system reacts during crawling behavior and tactile stimulations. We

40   conducted calcium imaging experiments on dissections of the isolated nervous system (missing all

41   sensory input) and found spontaneous rhythmic wave pattern of neuronal activity in VUM neuron

42   clusters over the range of thoracic and abdominal neuromeres in the VNC. In contrast, *in vivo*

43   preparations (semi-intact animals, receiving sensory input) did not reveal such spontaneous rhythmic

44   pattern. However, tactile stimulations activated different clusters of the VUM neuron system

45   simultaneously in these preparations. The activation intensity of VUM neurons in the VNC was

46   correlated with the location and degree of body wall stimulation. While VUM neuron cluster near the

47   respective location of body wall stimulation were less activated more distant cluster showed stronger

48   activation. Repeated gentle touch stimulations led to decreased response intensities, repeated harsh

49   stimulations resulted in increasing intensities over trials. Optophysiological signals correlated highly

50   with crawling behavior in freely moving larvae stimulated similarly. We conclude that the

51   octopaminergic system is strongly coupled to the neuronal pattern generator of crawling movements

52   and that it is simultaneously activated by physical stimulation, rather intensity than sequential coded.

53   We hope that our work raises the interest in whole biogenic network activity and shows that

54   octopamine release does not only underlie "the more the better" principle but instead has a more

55   complex function in control and modulation of insect's locomotion.

Introduction

59   Insects use information about their environment and internal physiological states to execute fast,

60   reflex-like sensory-guided behavior. In contrast to goal-directed behavior which depends on

61   multimodal integration and memory in higher brain centers of the supraoesophageal (cerebral)

62   ganglion (hereafter referred to as 'brain') some autonomous rhythmic behaviors such as crawling,

63   walking, swimming or flying are generated brain-independently in the nerve cord and the gnathal

64   ganglia. Here, neuronal networks, including motoneurons that innervate the muscles as output

65   elements, are responsible for the execution of coordinated behaviors such as locomotion. While in the

66   intact animal, central pattern generators (CPG) are modulated by sensory input and the regulatory

67   control of the brain, in isolated ventral cords they can work autonomously. The importance and

68   function of neuronal CPGs for locomotor behavior in *Drosophila* larvae is discussed extensively (Fox *et*

69   *al.*, 2006; Song *et al.*, 2007; Xiang *et al.*, 2010; Berni *et al.*, 2012; Gomez-Marin & Louis, 2012). The

70   modulation of CPGs by biogenic amines adds another important variable to the subject. In parallel to

71   the motor network a small-sized network of octopaminergic neurons release octopamine (OA) onto

72   neuromuscular junctions (NMJs) and potentially onto synapses within CPGs to modulate synaptic

73   transmission and other physiological processes important for motor behaviors. In large insects such as

74   locusts, the octopaminergic neurons of a thoracic ganglion, for example, are divided into different

75   subpopulations with different morphologies (Watson, 1984; Duch *et al.*, 1999; Kononenko & Pflüger,

76   2007) and functions (Burrows & Pflüger, 1995; Baudoux *et al.*, 1998; Duch & Pflüger, 1999). Techniques

77   to alter the concentrations of biogenic amines were used to exploit effects on individual or small

78   groups of neurons and the behavioral consequences. However, how whole neuronal aminergic

79   networks in insects are functioning system-wide is less investigated and difficult to achieve with

80   electrophysiological recording methods but, as demonstrated here, possible by optophysiological

81   methods.

82   Octopamine is a member of the phenolamine family, synthesized from the amino acid L-

83   tyrosine functioning as a neurotransmitter, a neuromodulator and a neurohormone in invertebrates.

84   Based on structural and functional similarities, the monoamine OA and its direct precursor tyramine

85   (TA) constitute the invertebrate counterpart of the vertebrate's norepinephrine and dopamine system

86   (Roeder, 2005; Vömel & Wegener, 2008; Selcho *et al.*, 2012). Octopamine was first found and

87   described in the salivary glands of octopoda (Erspamer, 1948) and was later comprehensively studied

88   in arthropods and insects where it plays an important role in a variety of behavioral contexts (Roeder

89   *et al.*, 2003; Roeder, 2005; Farooqui, 2012). It acts in the central as well as in the peripheral nervous

90   system where it is released mainly under stress conditions, e.g. starvation (Wicher, 2007; Suo *et al.*,

91   2009), aggression (Baier *et al.*, 2002; Stevenson *et al.*, 2005) or foraging (Fussnecker *et al.*, 2006;

92   Scheiner *et al.*, 2006). Among its versatile functions, OA can alter the efficacy of neuromuscular

93   transmission (Walther & Zittlau, 1998), changing energy metabolism (Mentel *et al.*, 2003), having

94   hyperglycaemic action (Candy, 1978; Zeng *et al.*, 1996) and inhibiting myogenic oviduct rhythms,

95   accessory hearts and gut movements (Orchard & Lange, 1986; Papaefthmiou & Theophilidis, 2001). In

96   addition, it is discussed as the "reward transmitter" of insects in associative learning paradigms

97   (Hammer, 1993; Hammer & Menzel, 1998; Schroll *et al.*, 2006; Waddell, 2013). Importantly, OA was

98   found to be involved in the activity and modulation of central networks for locomotion (Hoyle & Dagan,

99   1978; Sombati & Hoyle, 1984; Duch & Pflüger, 1999; Fox *et al.*, 2006; Pflüger & Duch, 2011). Its action

100   had been studied extensively in large hemimetabolous insects such as locusts (for review see Bräunig

101   and Pflüger (2001) but a number of studies were also concerned with the holometabolous *Drosophila*

102   fly (Hoyer *et al.*, 2008; Vömel & Wegener, 2008; Zhou *et al.*, 2008; Busch *et al.*, 2009; Busch &

103   Tanimoto, 2010; Selcho *et al.*, 2014; Pauls *et al.*, 2018), and the role of both amines, OA and TA in larval

104   crawling (Selcho *et al.*, 2012) or OA in flight (Brembs *et al.*, 2007).

105   Common in insects, octopamine is released by a special class of neurons with bilaterally

106   symmetrical axons in the ventral nerve cord and gnathal ganglia. These neurons have dorsal or ventral

107   unpaired median cell bodies which, therefore, were called DUM or VUM neurons, respectively

108   (Plotnikova, 1969; Crossman *et al.*, 1971; Hoyle, 1974; 1975; Hoyle & Dagan, 1978; Arikawa *et al.*, 1984;

109   Bräunig & Pflüger, 2001). In locusts, these neurons fall into subpopulations which are differentially

110   recruited during various motor tasks (Burrows & Pflüger, 1995; Baudoux & Burrows, 1998; Baudoux *et*

111   *al.*, 1998; Duch *et al.*, 1999; Duch & Pflüger, 1999). In stick insects they are recruited during walking

112   behavior (Mentel *et al.*, 2008) and descending VUM-neurons from the gnathal ganglion are involved

113   in sensory gating (Stolz *et al.*, 2019). However, in the fruit fly, *Drosophila melanogaster*, it is unknown

114   whether octopaminergic VUM neurons are also functionally subdivided during motor behavior.

115   *Drosophila's* 3rd instar larval developmental state offers an octopaminergic system easily accessible for

116   optophysiological investigations when compared to adult animals. Cell bodies of octopaminergic

117   neurons can be found in the brain lobes and in the ventral nerve cord (VNC). As the larval body, the

118   VNC is segmentally organized displaying three suboesophageal (s1-s3), three thoracic (t1-t3) and eight

119   abdominal neuromeres (a1-a8), plus a small terminal neuromere at the end (a9). Clusters of

120   octopaminergic cell bodies can be found in each neuromere. Thoracic and abdominal clusters can

121   contain paired (VPM; t1-t3, a1) and unpaired (VUM; t1-t3, a1-a9) ventromedial neurons. Only the

122   terminal neuromere possesses a dorsomedial cluster (DUM) (Vömel & Wegener, 2008; Selcho *et al.*,

123   2012) (Fig. 1A). The primary neurites of thoracic and abdominal VUM neurons are projecting first

124   dorsally and then bifurcate, projecting laterally and leaving the VNC via the peripheral nerve strands

125   (Fig. 3A and Suppl. Fig. 2A). The axonal VUM neuron projections target all the animal's body wall

126   muscles and modulate NMJ synapses by OA release (Monastirioti *et al.*, 1995; Monastirioti, 1999; Koon

127   *et al.*, 2011; Koon & Budnik, 2012). Therefore, in this study we attempt to monitor the combinatory

128   activity of the entire thoracic and abdominal population of VUM neurons in the VNC during larval

129   crawling behavior simultaneously by optophysiological methods.

130   *Drosophila's* 3rd instar larvae offer a simple behavioral repertoire including peristalsis (forward

131   and backward crawling), bending, turning and feeding (Green *et al.*, 1983; Fox *et al.*, 2006; Gomez-

132   Marin & Louis, 2012). They use crawling behavior to execute escape reactions, to access food, to avoid

133   competition and to find appropriate pupation areas. Forward crawling movements are initiated by the

134   elevation and forward shift of the head and thorax body segments. Simultaneously a forward directed

135   contraction wave starts traveling through the abdominal segments along the body axis from tail (body

136   segment A8/9) to head (body segment A1) (Dixit *et al.*, 2008; Lahiri *et al.*, 2011; Berni *et al.*, 2012;

137   Heckscher *et al.*, 2012). Backward movements are initiated by a retraction of the head and thorax

138   followed by a backward directed contraction wave traveling through the abdominal body segments

139   (Crisp *et al.*, 2008). All these behaviors are guided by sensory inputs, while the execution of movements

140   (crawling and turning) are autonomous behavioral patterns created within the segmental motor-

141   network of the nerve cord (Berni *et al.*, 2012). The larval body segments are targeted by these networks

142   via nerve strands connecting the central nervous system (CNS = brain lobes + VNC) with the body

143   periphery. These peripheral nerve strands carry not only motoneurons and efferent VUM neurons but

144   importantly also the afferences from sensory receptor neurons. However, it is uncertain how exactly

145   sensory input modulates the generation of rhythmic crawling behavior and, likewise, it remains an

146   unclarified question, if, how and where the octopaminergic system might be involved in such

147   modulation processes - only in the periphery or potentially also in the CNS?

148   In the present study we used tactile stimulations of different degrees in strength to initiate

149   peristaltic crawling movements and to activate the animal's octopaminergic system. By gentle and

150   strong (noxious) physical touches against the external side of the animal's body wall we aimed to

151   activate different types of mechanoreceptors and studied the modulatory involvement of the

152   octopaminergic system on the escape crawling behavior of the fruit fly's 3rd instar larvae. We used

153   calcium imaging techniques to examine the combinatory VUM neuron cluster activity in the VNC.

154

Results

156   In different experimental approaches we investigated if and how octopaminergic neurons are involved

157   in pattern generators responsible for larval crawling behavior in *Drosophila melanogaster*. Therefore,

158   we used calcium imaging techniques to record neuronal activity signals from isolated (deafferented)

159   CNS dissections in **Experiment 1** (n = 17) of 3rd instar *Drosophila melanogaster* larvae expressing

160   GCaMP3.0 in octopaminergic neurons (Tdc2-GAL4/UAS-GCaMP3.0). Furthermore, we used the same

161   techniques and transgenic animals to record from semi intact *in vivo* preparations of the CNS in

162   **Experiment 2 and 3** (n > 500). In these experiments ~60% of the isolated CNS dissections (n = 10) and

163   in ~5% of the *in vivo* preparations (n = 27) we could measure changes in calcium concentrations

164   signaling neuronal activity eligible for data analysis. In addition, we conducted behavioral open surface

165   experiments observing the crawling performance of 3rd instar larvae (n = 148) before and after tactile

166   stimulations in **Experiment 4**.

167

168   ***Experiment 1. Spontaneous activity pattern in the VUM neuron system of isolated (deafferented)***

169   ***CNS preparations.*** We started our investigation by scrutinizing the role of octopaminergic neurons in

170   active central pattern generators (CPG) of the isolated CNS. The isolation of the brain and ventral nerve

171   cord prohibits any influence of afferent sensory input from the periphery on CPGs and permits only

172   neuronal mechanisms and connections within the CNS. Besides arrhythmic neuronal activity,

173   deafferented CNS dissections showed rhythmic wave pattern (posterior to anterior and *vice versa*)

174   restricted to the thoracic and abdominal VUM neuron system in the VNC (Fig. 1B and Suppl. Movies 1

175   and 2). Rhythmic wave patterns are an indication for a possible participation of the octopaminergic

176   system in larval crawling behavior since similar spatio-temporal patterns were already found
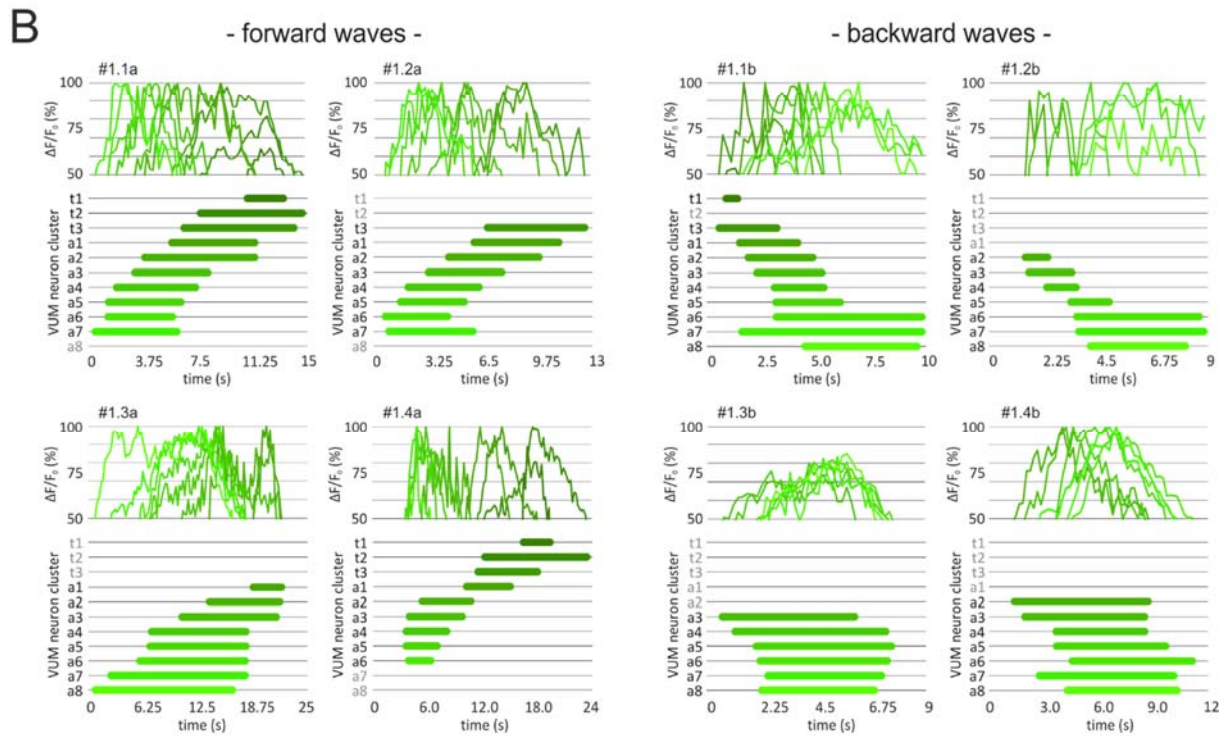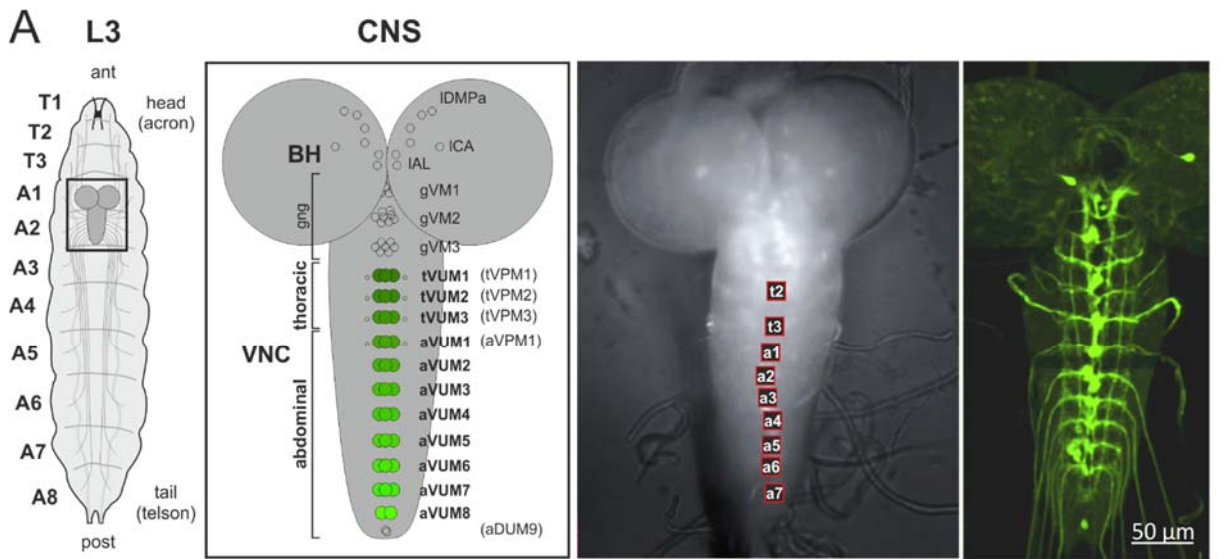
	forward waves	backward waves	average *forward* wave duration	average *backward* wave duration
VUM neuron pattern isolate CNS Tdc2-GCaMP3 (n = 10; T1-A8)	28	11	10.8 ± 4.8 s	8.3 ± 1.2 s
Motorneuron pattern isolate CNS OK371-GCaMP (n = 10; T3-A8/9)*	10	10	10.9 ± 6.0 s	5.3 ± 3.1 s

177   (*Pulver et al. - J Neurophysiol - 2015)

178   **Figure 1**. Spontaneously occurring activity wave pattern in octopaminergic VUM neuron cluster. Panel **A** shows the

179   segmented body (T1-A8) of a 3rd instar larvae and its CNS with neuronal projections innervating the body wall of each

180 hemisegment (*left*). The CNS consists of two brain hemispheres and one elongated VNC. Three octopaninergic cell body
181 cluster can be found in both brain hemispheres (lDMPa: larval anterior dorsomedial protocerebrum cluster; lCA: larval calyx
182 cluster; lAL: larval antennal lobe cluster; after (Selcho *et al.*, 2014)) and 15 cluster in the VNC, three of which can be found in
183 the gnathal (gVM1-3), three in the thoracic (tVUM1-3; tVPM1-3) and 9 in the abdominal neuromeres (aVUM1-8; aVPM1;
184 aDUM9). Our investigation concentrated on the thoracic (tVUM1-3) and abdominal cluster (aVUM1-8) colored in different
185 shades of green (*center left*). The anatomical grey scale image shows the ventral side of the brain. ROIs were set where cluster
186 could be identified based on GCaMP5 auto-fluorescence (red squares, 5 x 5 pixel). In the shown example cluster tVUM2-
187 aVUM7 (t2-a7) appeared in the focal plane and could be analyzed for fluorescence changes during imaging measurements
188 (*center right*). The confocal microscopy image shows cluster and bilateral axonal projections of VUM neurons leaving each
189 thoracic and abdominal VNC neuromere via paired nerve strands towards their appointed body segments (*right*). In panel **B**
190 spontaneously occurring forward (*left*) and backward (*right*) wave pattern in the isolated brain preparations are visualized.
191 Line graphs signify fluorescence changes over time passing the half maximum (50%) intensity threshold for each cluster.
192 Beneath, horizontal bar graphs signify only the time fluorescence was passing the 50% threshold in each individual cluster to
193 clearly visualize wave pattern. The table in panel **C** compares wave durations of forward and backward VUM neuron pattern
194 with fictive locomotor pattern found in motoneurons of isolated brain preparations in *Drosophila* larvae by (Pulver *et al.*,
195 2015).

196

197 in VNC motoneurons for a fictive crawling pattern (Pulver *et al.*, 2015). From 10 larval CNS dissections
198 we analyzed 28 forward and 11 backward waves. Sixty percent of the animals showed both forward
199 and backward waves whereas 40% showed only forward waves. Their occurrence was irregular and, in
200 some cases, overlapping meaning that a new wave was initiated already before the preceding one was
201 terminated. The average wave time lasted 9.8 sec ± 4.4 s.d. with forward waves being slightly slower
202 (10.8 sec ± 4.8 s.d.) than backward waves (8.3 sec ± 1.2 s.d.) (unpaired t-test, p = 0.039) (Fig. 1C). The
203 average VUM neuron activity duration for individual clusters was found 4.2 sec ± 2.5 s.d. In one
204 exceptional case we were able to see activation pattern beyond thoracic and abdominal clusters in the
205 gnathal ganglia cluster and the brain cluster. However, these activations could not be assigned to be
206 part of any wave pattern. After recordings of spontaneous activity, we pharmacologically induced VUM
207 neuron activity by applying pilocarpine (a muscarinic acetylcholine receptor agonist) to the CNS
208 dissections. Although pilocarpine induces activity pattern in the CNS of many insects (Ryckebusch &
209 Laurent, 1993; Büschges *et al.*, 1995; Johnston & Levine, 1996; Johnston *et al.*, 1999) its application
210 neither changed the average wave time durations (10.3 sec ± 4.6 s.d.) nor increased the average cluster
211 activity duration (4.7 sec ± 2.6 s.d.) (unpaired t-test, p > 0.05 in both cases). The maximum change in
212 fluorescence intensity during wave pattern reached a value of 23.52 ± 9.3 (change in absolute grey
213 scale values, calculated against the background).

214

215 ***Experiment 2. Activity pattern in the VUM neuron system of in vivo preparations.*** In contrast to
216 *Experiment 1* we were not able to see spontaneous neuronal activity pattern in the VUM neuron
217 system of *in vivo* preparations. *In vivo* preparations of larvae had the brain and all nerve cords with

218   afferent and efferent neurons completely intact. These larvae were able to execute stationary crawling

219   movements in forward and backward direction while being held in place by pins at the anterior head
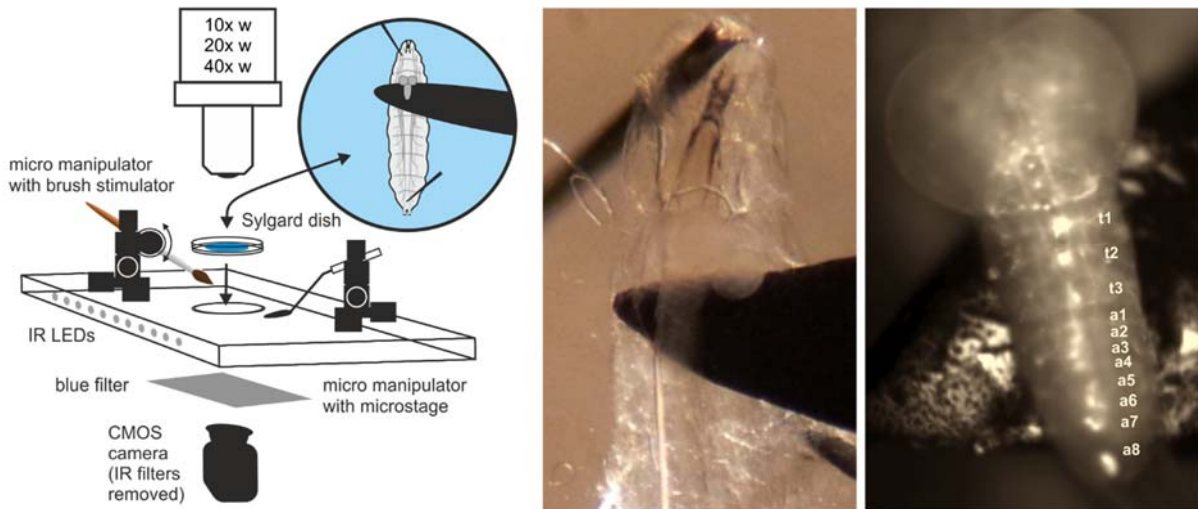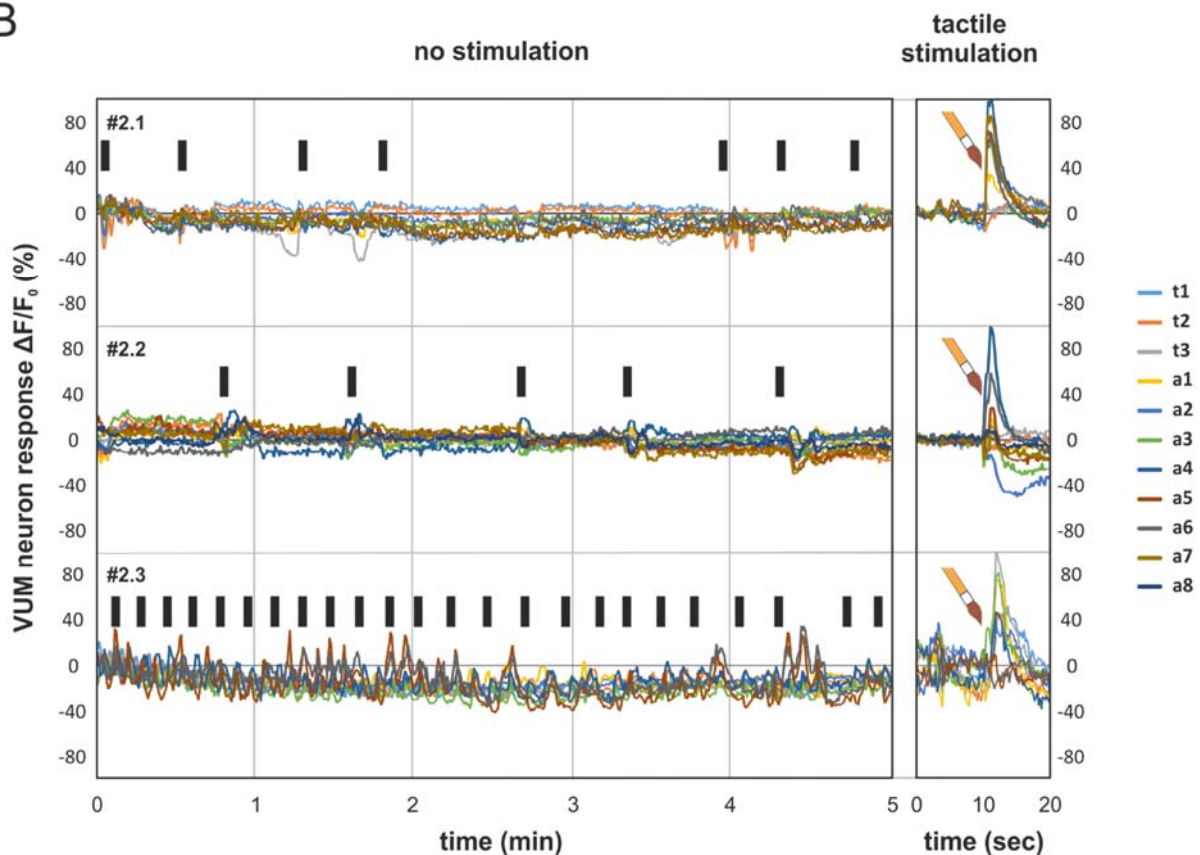
220

221   **Figure 2.** Activity pattern in the VUM neuron system of in vivo preparations. The sketch in panel **A** shows important parts of

222   the experimental setup (*left*). Third instar larva were pinned onto a Sylgard dish and were covered by saline. The dish was

223   placed under the microscope on a acryl glass platform equipped with two micromanipulators for stimulators and the

224   microstage. The transparent platform had infrared (IR) LEDs and a CMOS camera allowing for video capturing of larval

225   movements in the dark. The microstage was carefully positioned under the VNC (*center*) and the fluorescence of identified

226   VUM neuron cluster were imaged (*right*). Panel **B** shows calcium imaging recordings over 5 minutes of VUM neuron cluster

227   in the VNC of unstimulated larvae (*left*). Black bars signify larval crawling behavior confirmed by control ROIs outside the VNC

228   in calcium imaging analysis and video capturing. Unstimulated larvae showed no consistent VUM neuron responses correlated

229   to crawling movements. Sixty seconds after each 5 minute recording a new recording started comprising a tactile brush

230   stimulation after 10 seconds (*right*). Tactile brush stimulations resulted in strong VUM neuron responses in many abdominal

231   and thoracic cluster.

232

233   segment and the telson (Fig. 2A and Suppl. Movie 3). These stationary movements occurred

234   spontaneously without any experimental stimulations. Measured over 5 minutes, crawling or other

235   behavioral movements were not accompanied by related neuronal activity wave pattern in the VUM

236   neuron system as found in deafferented CNSs of *Experiment 1* (Fig. 2B, *left panel*). Thus, sensory

237   feedback from stationary crawling movements is not sufficient to trigger VUM neuron activity or wave

238   pattern in *Drosophila* larvae.

239   Conversely, when the body wall of a larva was stimulated by harsh tactile brush stimulation at the

240   posterior end of the larvae the thoracic and abdominal VUM neuron system responded strongly.

241   However, stimulations did not initiate wave pattern activity but led to strong simultaneous activity (in

242   the boundaries of our time resolution given by the calcium sensor GCaMP3, $t^{1/2}$ = 83 ± 2 ms) (Fig.2,

243   *right panel*). These results were found consistently between animals. The maximum change in

244   fluorescence intensity after harsh brush stimulation reached on average a value of 143.91 ± 28.27

245   (change in absolute grey scale values, calculated against the background).

246   In very rare cases pilocarpine application to intact brains (incubation of 5-10 min) led to flicker (on-

247   off) activity in individual VUM neuron cell bodies lacking any coordination within the same or between

248   different VUM neuron cluster (Suppl. Movies 4 and 5). Thus, individual VUM neurons have the

249   potential to show independent activity from VUM neurons of the same or other cluster. However, the

250   phenomenon of individual VUM neuron activity appeared only after pharmaceutical application or

251   after damaging neuronal tissue during dissections.

252

253   ***Experiment 3. VUM neuron pattern in response to consecutive tactile stimulations.*** To reveal how

254   stable and consistent simultaneous VUM neuron responses occur after tactile stimulation we applied

255   multiple stimulations within each experimental run. In addition to harsh brush stimulations (Fig. 3*, in*

256   *shades of red* and Suppl. Movie 6) we also applied gentle rod stimulations (Fig. 3*, in shades of blue* and

257   Suppl. Movie 7) to see if and how the VUM neuron system responds to different degrees of tactile

258   stimulation and body wall deflections. Larvae were stimulated three times in each experimental run

259   after 10, 30 and 50 seconds (20 seconds inter trial interval, ITI) either at posterior or anterior body

260   segments.

261   Posterior brush stimulations elicited strong and slightly increasing fluorescence responses over

262   successive stimulations without total recovery of baseline fluorescence within 20 seconds ITIs (Fig. 3B,

263   *left panel* and Suppl. Movie 8). For data analysis responses were averaged over 10 seconds after each

264   stimulation and for each VUM neuron cluster. Although simultaneously active individual cluster

265   differed in response strength, cluster aVUM8 (a8) - the cluster which gets sensory input from body
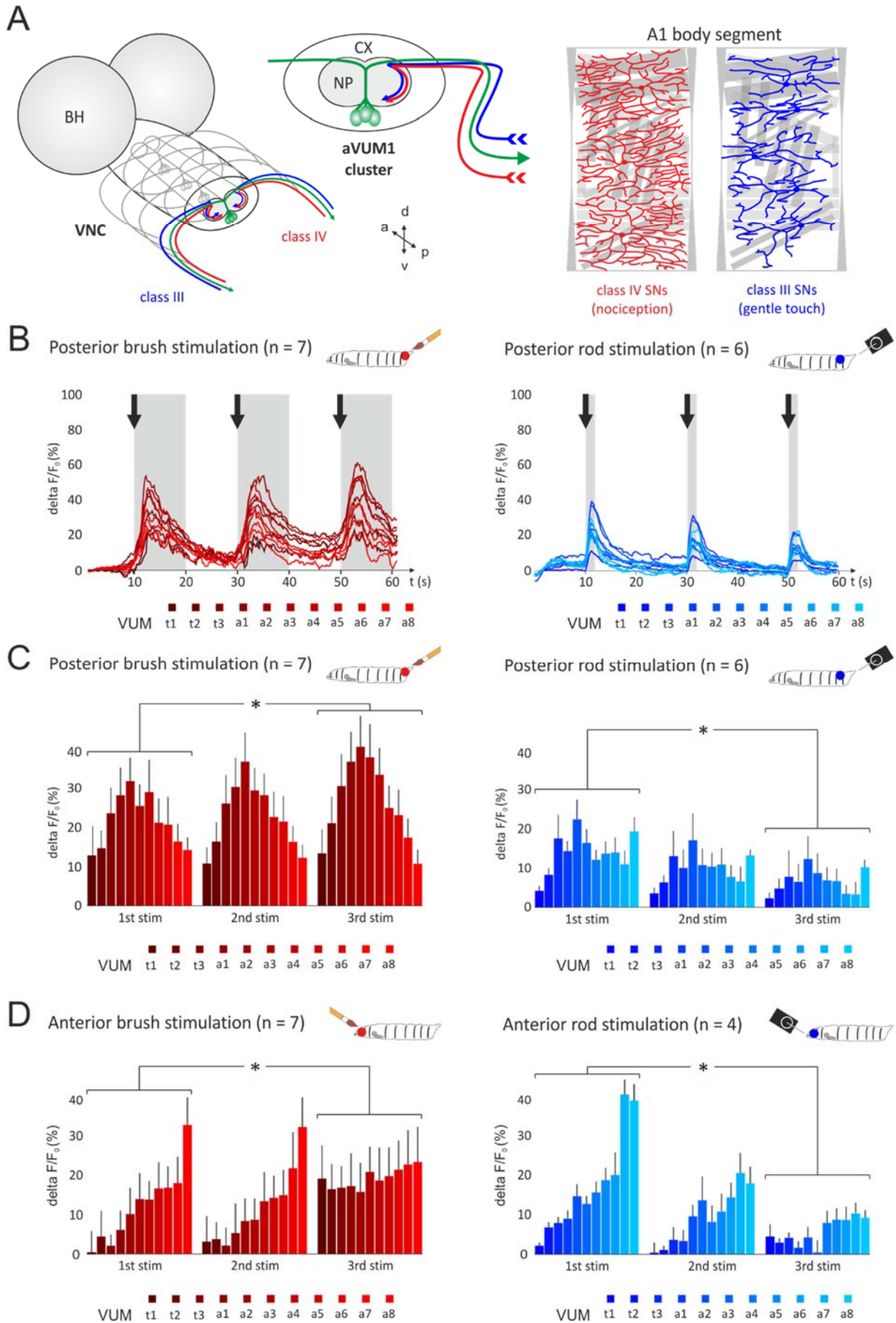
267 **Figure 3.** VUM neuron pattern in response to consecutive tactile stimulations. **A** Schematic drawing of the paired brain
268 hemispheres and the VNC cut in the axial plane at abdominal VUM neuron cluster a1 (aVUM1). Three thoracic cluster (tVUM1-
269 3) are shown in grey whereas abdominal cluster a1 is shown in green (*left*). VUM neuron cell bodies are located ventral medial
270 and their primary neurite bifurcates dorsally descending axonal projections to corresponding body segments and NMJs.
271 Ascending class III and class IV sensory neurons are depicted in blue and red, respectively. Class III and class IV neurons entre
272 the neuropile at the dorsal part and project to their ventral target regions (*center*). Covering each body hemisegment harsh
273 and gentle touch stimulations are perceived by class IV and class III sensory neurons, respectively (*right*). **B** Harsh (*left, in*
274 *shades of red*) and gentle (*right, in shades of blue*) tactile stimulation of the larval body wall elicit different response activities
275 in VUM neurons. The graphs are showing activation of identified thoracic and abdominal VUM neuron cluster over 60
276 seconds. Larvae were stimulated at the posterior end of the body either harshly with a brush (*left*) or gently with a small
277 metal rod (*right*) three times in each experimental run after 10, 30 and 50 seconds (black arrows). Brush stimulations elicited
278 strong and slightly increasing fluorescence responses over successive stimulations without total recovery of baseline
279 fluorescence within 20 seconds after stimulations. Rod stimulations in contrast elicited strong but decreasing responses over
280 successive stimulations. **C** Quantification of individual cluster responses to posterior brush stimulation (*left*) and posterior
281 rod stimulation (right). After each stimulation responses to brush or rod stimulations were averaged over 50 (10 seconds) or
282 10 (2 seconds) consecutively imaged frames, respectively (as indicated by the grey boxes in B). A statistically significant
283 difference between responses (over all 11 cluster) was found after the first and the third stimulation. **D** Quantification of
284 individual cluster responses to anterior brush stimulation (*left*) and anterior rod stimulation (right) A statistically significant
285 difference between responses (over all 11 cluster) was found after the first and the third stimulation. Error bars represent
286 standard errors.

287

288 segment A8 where the animal was stimulated the most - showed the lowest response intensity of all
289 abdominal clusters. Cluster aVUM2 (a2) showed highest response intensity and all other abdominal
290 clusters in between showed increasing intensities. However, after the peak response in cluster a2
291 response intensities decreased again in cluster a1, t3, t2 and t1. This pattern was consistently found in
292 all consecutive stimulations. The average response intensity over all clusters were statistically
293 compared between first, second and third stimulation (1st stim, 2nd stim and 3rd stim, respectively).
294 Paired t-tests found a significant increase between responses after the 1st and 3rd stimulation ($p =$
295 0.017; n = 7) (Fig. 3C, *left panel*).

296   Anterior brush stimulations elicited also strong and slightly increasing fluorescence responses over
297 successive stimulations, however the simultaneous VUM neuron response pattern differed from
298 posterior stimulations. Anterior brush stimulations led to weak responses in thoracic cluster and
299 produced increasing response strength from abdominal cluster aVUM1 (a1) to a maximum in
300 abdominal cluster aVUM8 (a8). Statistical comparison between responses after 1st, 2nd and 3rd
301 stimulation using paired t-tests showed a significant increase between responses after the 1st and 3rd
302 stimulation ($p = 0.010$; n = 7) (Fig. 3D, *left panel*). The maximum change in fluorescence intensity after
303 tactile brush stimulation (including posterior and anterior stimulations) reached an average value of
304 104.48 ± 50.79 (change in absolute grey scale values, calculated against the background).

305   Posterior rod stimulations in contrast, elicited strong but decreasing responses over successive
306   stimulations (Fig. 3B, *right panel* and Suppl. Movie 9). Responses were averaged over 2 seconds after
307   each stimulation and for each VUM neuron cluster. Again, VUM neurons responded simultaneously
308   and the response strength differed between individual cluster. Cluster aVUM8 (a7) - the cluster which
309   gets sensory input from body segment A7 where these animals were stimulated - showed the lowest
310   response intensity of abdominal cluster. Cluster aVUM2 (a2) showed highest response intensity and
311   intensities decreased again in cluster a1, t3, t2 and t1. Paired t-tests found a significant decrease
312   between responses after the 1st and 3rd stimulation (p < 0.001; n = 6) (Fig. 3C, *right panel*).

313   As for brush stimulations anterior rod stimulations produced weakest responses in anterior cluster
314   and strongest responses in posterior cluster but showed decreasing responses over successive
315   stimulations. Paired t-tests found a significant decrease between responses after the 1st and 3rd
316   stimulation (p = 0.011; n = 4) (Fig. 3D, *right panel*). The maximum change in fluorescence intensity after
317   tactile rod stimulation (including posterior and anterior stimulations) reached an average value of
318   52.23 ± 40.61 (change in absolute grey scale values, calculated against the background).

319   Altogether, VUM neurons showed consistently weaker responses in those clusters which are getting
320   sensory input from stimulated body segments and stronger responses in clusters getting input from
321   segments further away from stimulated segments.

322

323   ***Experiment 4. Tactile stimulation of freely moving larvae - a correlation between optophysiological***
324   ***recordings and behavioral observation data***. In a last step we wanted to investigate if tactile
325   stimulations and hence a change in VUM neuron activity (as shown in ***Exp. 2*** and ***Exp. 3***) have any effect
326   on the larval crawling behavior. Since VUM neuron activity results in a release of octopamine at the
327   target areas of axonal projections, the NMJs and muscle fibers (Fig. 4A), synaptic properties and muscle
328   conditions are expected to be altered leading to changes in crawling dynamics (compare Koon et al.
329   2011).

330   In very simplistic behavioral assays we concentrated on changes in the crawling frequencies of larvae
331   after repeated tactile stimulations of different degrees (gentle rod and harsh brush stimulations). Both
332   types of stimulations were conducted in respective experimental groups. Before stimulations larvae in
333   the gentle rod stimulation group displayed undisturbed foraging behavior with a crawling frequency
334   of 0.90 Hz during 20 seconds (n = 65). After three successive stimulations with an inter trial interval
335   (ITI) of 20 seconds frequencies first increased to 1.05 Hz and then decreased again to 0.98 Hz and 0.96
336   Hz after the 1st, 2nd and 3rd stimulation, respectively (Suppl. Fig. 3A). Larvae in the harsh brush
337   stimulation group initially showed a crawling frequency of 0.71 Hz before stimulations (n = 83). After
338   successive stimulations frequencies increased to 0.81 Hz, 0.88 Hz and 0.90 Hz after the 1st, 2nd and 3rd
339   stimulation, respectively (Suppl. Fig. 3B).

340   To compensate for the difference in initial crawling frequencies (before 1st stimulation) between

341   experimental groups a crawling index was calculated before statistical comparisons were made. For

342   index calculations in both experimental groups, the number of crawling events after each stimulation

343
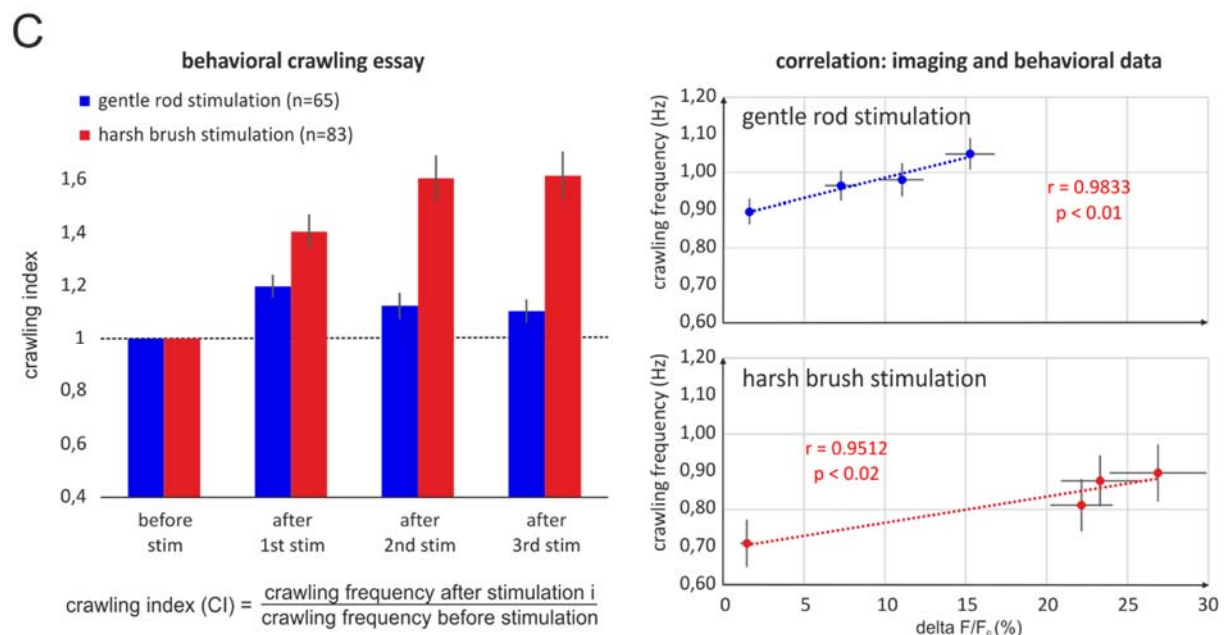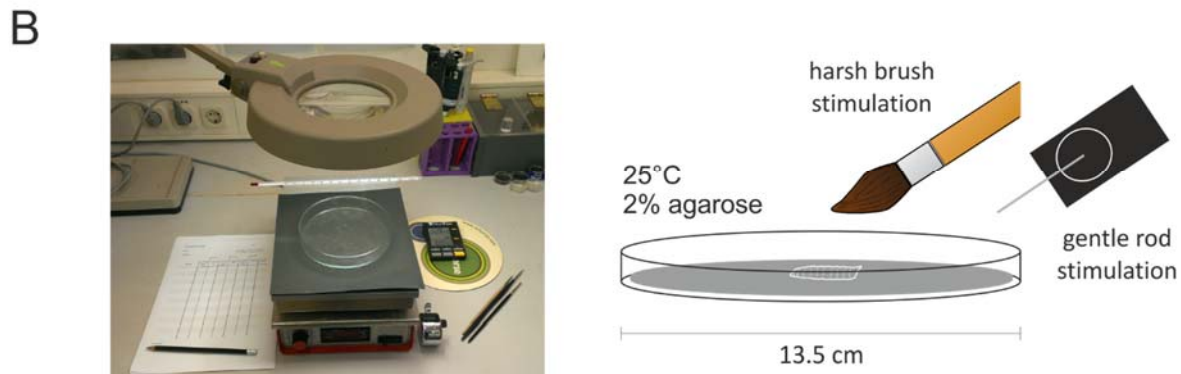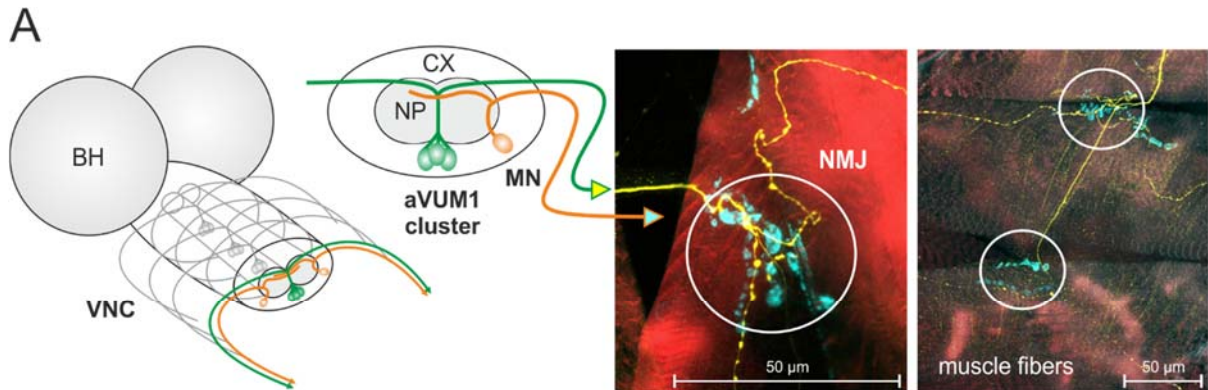
344   **Figure 4.** Tactile stimulation of freely behaving larvae. **A** Schematic drawing of the paired brain hemispheres and the VNC cut

345   in the axial plane at abdominal VUM neuron cluster a1 (aVUM1) (left). Descending axonal projections of aVUM1 neurons

346   (green) and motoneurons (orange) leave the VNC in parallel via the same nerve strands bilaterally and project to muscle

347   fibers of their corresponding body segment A1. VUM neurons target NMJs at multiple muscle fibers and have lateral Type II

348   projections along the muscle fibers (*right, confocal images*). In confocal images VUM neurons are depicted in yellow, NMJs

349   in cyan and muscle fibers (actin filaments) in red. **B** In behavioral essays larvae were released in the center of a glass dish

350   cast with 2% agarose. The dish was placed on a temperature controlled plate and behavioral performances were observed

351   under a magnification glass (2x). Crawling events were counted before and after harsh brush and gentle rod stimulations in

352   respective experimental groups. **C** Bar graphs show the crawling performance index of larvae during a time period of 20

353   seconds before any stimulation and 20 seconds after each of the three successive stimulations (ITI of 20 seconds). In blue and

354   red responses to gentle rod (n = 65) and harsh brush (n = 83) stimulations are given, respectively. Responses to gentle rod

355   stimulations increased the crawling frequency after the first stimulation but then decreased again after the second and third

356   stimulation. In contrast, responses after harsh brush stimulations show ever increasing crawling frequencies after each

357   stimulation (*left*). Correlation analysis between imaging and behavioral data were performed using linear regression analysis

358   and Pearson's correlation coefficients. Both data sets are highly correlated (*right*). Error bars represent standard errors.

359

360   were divided by the number of crawling events before the 1st stimulation. Therefore, controls before

361   stimulation have a crawling index of 1. After the 1st stimulation the index of both experimental groups

362   increased, however stronger in the harsh brush stimulation group (gentle rod: 1.20; harsh brush: 1.40).

363   After the 2nd stimulation the index for the gentle rod stimulation group dropped to 1.12 whereas the

364   index for the harsh brush stimulation group further increased to 1.60. After the 3rd and last stimulation

365   the index for the gentle rod stimulation group further decreased to 1.10 and it further increased in the

366   harsh brush stimulation group to 1.61 (Fig. 4C, *left panel*, gentle rod group in blue and harsh brush

367   group in red).

368   For correlation analysis between behavioral crawling frequencies and optophysiological signal

369   intensities (averaged over all measured VUM neuron cluster) in both experimental groups we used

370   linear regression analysis and Pearson's correlation coefficients. Analysis revealed a significant

371   correlation between both data sets in both experimental groups (gentle rod: r = 0.98, p < 0.01; harsh

372   brush: r = 0.95, p < 0.02) (Fig. 4C, *right panel*). Therefore, successive tactile stimulations of different

373   degrees lead to characteristic adaptation of both the neuronal VUM neuron activity and the crawling

374   behavior. In case of gentle rod stimulations this means habituation after an initial increase and

375   sensitization in case of harsh brush stimulations.

376

Discussion

378   Motivated by the many electrophysiological studies concentrating on individual or small populations

379   of VUM neurons simultaneously, we wanted to reveal how the VUM neuron system reacts during

380   crawling behavior as an entity. Therefore, we conducted calcium imaging experiments on the nervous

381   system of *Drosophila* larvae. In isolated larval CNS dissections that do not receive sensory input we

382   found spontaneous rhythmic wave pattern of neuronal activity in VUM neuron clusters over the range

383   of thoracic and abdominal neuromeres in the VNC. Surprisingly, *in vivo* preparations that receive

384   sensory input did not show such spontaneous rhythmic pattern, no matter if the animals were

385   executing crawling movements or not. However, tactile stimulations activated different clusters of the

386   VUM neuron system simultaneously while the activation intensity was correlated with the location and

387   degree of body wall stimulation. While the response of VUM neurons in stimulated neuromeres was

388   low, it increased in distant neuromeres. Moreover, the response intensities to repeated gentle touch

389   stimulations decreased, while they increased with repeated harsh stimulations over trials. The

390   optophysiological signals correlated highly with crawling behavior in freely moving larvae stimulated

391   similarly with gentle and harsh touches.

392   VUM neuron patterns found in our isolated CNS preparations were very similar to fictive crawling

393   patterns in motoneurons of deafferented larval CNS of *Drosophila melanogaster* (Pulver *et al.*, 2015).

394   This suggests a possible coupling of VUM neurons to the central pattern generator for larval crawling

395   behavior. However, in many cases the isolated CNS produces rhythms only similar and not identical to

396   the ones of intact animals but if phase relations of antagonistic systems are retained, the respective

397   motor behavior of the isolated CNS is called "fictive". Thus, removing sensory organs could lead to

398   changes in the functional principles of the whole pattern generator (CPG + sensory organs) (Bässler,

399   1986). How sensory information from the periphery is processed in the VNC and the brain to allow

400   smooth locomotor behavior is still a matter of extensive research. Here we propose VUM neurons as

401   one possible system to modulate either indirectly the endogenous input or directly the central pattern

402   generating neurons as a response to external tactile stimulation of the body wall. Two scenarios can

403   be considered: first, tactile stimulation *triggers* the pattern generator provoking a reflex and second,

404   tactile stimulation *modulates* the frequency of the already oscillating pattern generator. Both

405   scenarios can be explained by an endogenous input gradually changed and pushed above threshold by

406   sensory and/or modulatory neurons (e.g. octopaminergic VUM neurons) without input from higher

407   brain centers. In this model, octopaminergic neurons would be involved in gating processes similar to

408   what has been found in stick insects (Stolz *et al.*, 2019) or, perhaps, in changes associated with an

409   animal being active and starting a dynamic period of behavior.

410

411   **Sequential modulation in VUM neuron cluster activity**

412   The repeated sequential activation patterns in isolated CNS could have been triggered by either a

413   sequential recruitment by neurons presynaptic to VUM neurons and/or by a delayed coupling between

414   clusters. Work on *Manduca sexta* larvae showed that fictive crawling motor patterns were

415   accompanied by rhythmic activation of unpaired median (UM) neurons in all segmental ganglia derived

416   partially from a source within the gnathal ganglion (Johnston & Levine, 1996; Johnston *et al.*, 1999).

417   Because of very short anterior-to-posterior activation delays (~10 ms) only one or few descending

418   neurons of the gnathal ganglion projecting posteriorly to all segmental ganglia could be responsible

419   for all efferent UM neuron inputs. However, the sequential activation in isolated CNS preparations of

420   *Manduca sexta* larvae appear much faster than those found in *Drosophila melanogaster* larvae

421   preparations. The reason for this could be differences in the network organization and/or neuronal

422 properties but is so far unknown. In strong contrast to our isolated CNS preparations, VUM neuron

423 activation in our *in vivo* experiments (whole animal with intact sensory system) was synchronous and

424 appeared only after tactile stimulation, not during crawling. A possible reason for that could be the

425 fixed position of the larvae allowing only stationary crawling movements. Importantly, under fixed

426 conditions VUM neuron activation appears rather intensity than sequentially modulated. (Hu *et al.*,

427 2017) identified a pair of interneurons (a08n) with their cell bodies located in abdominal neuromere

428 a8 and having ascending ramifications over all thoracic and abdominal neuromeres. These

429 ramifications were situated in very close vicinity to nociceptive receptor neuron axon terminals in the

430 VNC which can detect harsh mechanical stimulations of the larval body wall (class IV dendritic

431 arborization neurons, class IV da). Importantly, a08n neurons responded to an optogenetically

432 activation of these nociceptive receptor neurons. Thus, in principle, a08n neurons could spread

433 information of tactile stimulation over the VNC with minimal delay and activate almost simultaneously

434 a downstream octopaminergic network system wide. Although still unclear, mechanisms of an

435 intensity modulation by the VUM neuron system could lead, in theory, to an aminergic readout about

436 where and how strongly in the periphery the sensory system was activated, thus encoding a

437 somatotopic map of the larval body wall. If VUM neurons and motoneurons are integral parts of the

438 same pattern generator for fictive crawling behavior, it is noteworthy that simultaneous activity in

439 VUM neurons would lead to octopaminergic modulation at their target NMJs preceding motoneuronal

440 input at most of the body wall segments and muscles. This is however not contradictive because of the

441 long-lasting effect of octopamine, resulting e.g. in synapses being prepared beforehand the arrival of

442 neuronal input. The idea of a synchronous activation by a common interneuron is also promoted by

443 recordings after pilocarpine application in which we saw cluster and individual VUM neurons activated

444 individually. We expect subpopulations of VUM neurons to be recruited for the modulation of

445 asymmetric or other more complex rhythmic or singular muscle activation patterns (e.g. rolling,

446 turning or hunch behaviors) as already found in other insects (Duch & Pflüger, 1999; Pflüger & Duch,

447 2011). Furthermore, it would be most interesting to compare larval VUM neuron activity patterns with

448 patterns of octopaminergic neurons in the adult systems during e.g. walking and flight behavior.

449

450 **Intensity modulation in VUM neuron cluster activity**

451 The absence of successive VUM neuron cluster activity in *in vivo* preparations (animals perceiving

452 sensory feedback) promotes the idea that it is not essential for the execution of basic crawling

453 movements but, however, for their modulation. Simultaneous and intensity modulated VUM neuron

454 activity was induced by body wall stimulation. In the periphery, octopaminergic neurons innervate the

455 major part of body wall muscles (Monastirioti *et al.*, 1995) where octopamine increases presynaptic

456 vesicle release (Koon *et al.*, 2011) at neural muscular junctions (NMJs) and contractions directly of

457   body wall muscle fibers/cells (Ormerod *et al.*, 2013). Importantly, the effects are cell selective and

458   correlate with the distribution of octopamine receptors (El-Kholy *et al.*, 2015) on different muscles

459   within each body wall segment. Hence, octopamine has an important role as neuromodulator and a

460   great potential impact on the coordination of different transversal and longitudinal muscles important

461   for crawling activity (Ormerod *et al.*, 2018). Fox *et al.* (2006) revealed that mutants ($T\beta h^{nM18}$) with a

462   reduced level of octopamine and an increased level of tyramine exhibit fewer rhythmic neuronal bursts

463   in motoneurons associated with body wall contraction waves. The same mutant animals lack crawling

464   speed and make more pauses compared to wild type (Saraswati *et al.*, 2004; Schützler *et al.*, 2019).

465   Our findings show that activity within the abdominal and thoracic VUM neuron system in the CNS is

466   synchronous and intensity modulated as, in consequence, should be the octopamine release at NMJs

467   in the body wall at the periphery. Together these findings suggest that octopamine release is important

468   1) for the coordination of muscle activity within an individual body segment, and 2) for the

469   coordination between all body segments since octopamine is released in different intensities

470   depending on the segment's location. In our study octopamine was only released after physical

471   stimulation, an event which in the natural environment represent a potential threat to the animal and

472   should be behaviorally responded to with avoiding behaviors and an increased crawling speed for body

473   displacement. This hypothesis is confirmed by our open field crawling behavior experiments, in which

474   contraction frequencies increased after physical stimulations. This is consistent with the idea that

475   octopamine is released to meet the coordinatively more challenging needs of "high" speed crawling

476   movements. Conclusions about central and peripheral observations both strengthen our idea of

477   octopamine as integral part of the pattern generator and modulator which increases muscle

478   coordination and movement performance over all body segments. Sujkowski *et al.* (2017) reported

479   that octopaminergic neurons mediate exercise adaptations increasing endurance of e.g. flight and

480   climbing performances in adult *Drosophila* flies. In this case adaptations were not limited only to

481   skeletal muscles but also e.g. to cardiac stress resistance. Octopamine mutants are also more

482   vulnerable to environmental stress (Chentsova *et al.*, 2002) while wildtype flies increase octopamine

483   levels in response (Hirashima *et al.*, 2000) suggesting that the effects are not only local but also

484   systemic adapting the whole system to higher performances. Future studies on the effects of

485   octopamine release like the coordination of muscles and body wall segments in the periphery, as well

486   as central effects and systemic adaptation are needed to fully evaluate the specific role of octopamine

487   and other neuromodulators and neuropeptides in larval and adult behavior (Ormerod *et al.*, 2018).

488

489   **VUM neuron responses in multiple trial stimulations**

490   The induction of multiple tactile stimulations of two different intensities changed VUM neuron

491   response patterns differently over trials. Different intensities of tactile stimulation activated probably

492 two different classes of sensory neurons (class III and IV da neurons) resulting in different VUM neuron

493 behaviors. Multiple gentle rod stimulations provoked initially an increase in VUM neuron activity after

494 the first trial which decreased and adapted quickly in consecutive stimulations. However, on a different

495 time scale this provides a similar effect as found by (Yan *et al.*, 2013) for class III da neurons which

496 showed a quick adaptation to prolonged gentle touch stimulation. Therefore, the adaptation effect

497 found in VUM neuron responses is probably caused by sensory input from adapting class III da sensory

498 neurons. To what degree a downstream network and the VUM neurons themselves are involved in

499 adaptation effects is unclear and needs further investigation. Harsh brush stimulations provoked

500 initially a comparable increase in VUM neuron activity, however, after repeated stimulations we found

501 VUM neuron activity increased rather than decreased. Because of the long livability of increased

502 calcium levels, we think that brush stimulations are perceived by class IV da sensory neurons sensitive

503 to noxious stimuli. Long lasting calcium increase indicates a mechanism to down regulate the neuronal

504 activity threshold and thereby an increase of excitability and sensitivity. Since octopamine release at

505 the NMJs increases the efficacy of synaptic transmission, a repeated noxious stimulation is responded

506 by a continual increase of octopamine release, and an ever facilitated transmission at the NMJs.

507 Additionally, it appears that a repetitive noxious stimulation of constant intensity can result in an

508 increasing response strength of nociceptive neurons (centrally mediated sensitization) leading to even

509 stronger escape behaviors after a second or a third noxious stimulation (Walters *et al.*, 2001; Ji *et al.*,

510 2003; Hu *et al.*, 2017; Tabuena *et al.*, 2017). Such an enhancer effect could be realized not only by

511 increased sensitivity of nociceptors but also within downstream interneurons or parallel VUM neurons.

512 Our behavioral data strengthens these interpretations since the same stimulations used to activate the

513 VUM neuron system in imaging recordings were used to stimulate freely crawling larvae. Responses to

514 multiple trial gentle rod and harsh brush stimulations followed exactly the same response pattern as

515 VUM neurons did. Initial stimulations increased crawling frequencies for both kinds of stimulations,

516 however, after the second and third rod stimulation crawling frequencies decreased whereas

517 frequencies after brush stimulations increased. The strong correlation of optophysiological and

518 behavioral data is striking and promotes the idea of a direct link between them.

519

Material & Methods

521 ***Animals and dissection.*** We used transgenic 3rd instar larvae of *Drosophila melanogaster* expressing

522 the calcium detector GCaMP3.0 in Tdc2 positive neurons (homozygous Tdc2-GAL4/UAS-GCaMP3.0)

523 allowing optophysiological activity surveillance of tyraminergic/octopaminergic neurons. GCaMP3 rise

524 half-life time $t^{1/2}$ = 83 ± 2 ms; decay half-life time $t^{1/2}$ or tau τ = 610 ± 32 ms (Tian *et al.*, 2009). Flies

525 were reared at 25°C and raised on standard cornmeal/molasses media, at a 12/12 h light/dark cycle.

526 For isolated brain imaging experiments larvae were dissected in cooled saline (85 mM NaCl, 20 mM

527   KCl, 4 mM MgCl2, 2 mM CaCl2, 10 mM HEPES, 20 mM Sucrose in Aqua dest., pH 7.25) using forceps to

528   extract the CNS from the body. Briefly, we held the larvae in place by one pair of forceps gripping it

529   halfway down its body length and extracting the CNS by pulling at the mouth hooks with a second pair

530   of forceps. After cleaning the brain tissue, it was pinned onto a Sylgard dish (Fig. 1A). For *in vivo* imaging

531   experiments 3rd instar larvae were anesthetized on ice before being pinned onto a Sylgard dish using

532   one pin at the anterior head segment and a second pin at the telson (Fig. 2). In that way body

533   displacement was restricted to peristaltic muscle contractions typical for larval crawling behavior.

534   Subsequently, larvae were dissected in cooled saline. For animal dissections a shallow dorsal incision

535   between the main tracheae was made starting between body segment A3 and A4 and running along

536   the dorsal midline longitudinally up to the head segment. The left and right body walls were pinned

537   flat to the bottom of the Sylgard dish. The esophagus, proventriculus and parts of the gut and glands

538   were removed. The brain lobes, VNC, and segmental nerves were left intact. The Sylgard dish was

539   transferred to a custom-made acryl glass microscope stage equipped with two micromanipulators

540   enabling the precise adjustment of tactile stimulators and the 'microstage' (Fig. 2A). The microstage,

541   a small custom-made metal spoon, was put under the VNC and was slightly elevated to minimize

542   artefacts during body wall stimulation or larval crawling movements. The surface of the spoon was

543   lacquered matt black to enhance contrast to the whitish transparent color of the VNC. The transparent

544   microscope stage was further equipped with infrared (IR) LEDs to allow for video recording of larval

545   movements in darkness from beneath and through the Sylgard dish. For video capturing we used a

546   CMOS camera (UCMOS 03100 KPA, ToupTek Photonics, Hangzhou, China) with its IR filter removed

547   and covered by a glass filter blocking wavelengths used for imaging recordings (Fig. 2A).

548

549   ***Stimulation.*** Mechanical stimulations of the larvae's body wall were applied by either a paint brush

550   (round, size 1) or a small metal rod (0.04 cm in diameter) at the anterior or at the posterior body

551   segments. In imaging experiments the brush was fixed to a rotating servomotor (SM-S2309S)

552   controlled by an Arduino UNO (microprocessor developer board) which was externally triggered by

553   imaging software. The brush was positioned laterally to the animal's body wall (not touching it). When

554   triggered it was swinging towards the body wall delivering a harsh mechanical (noxious) touch

555   deflecting the body wall more than 40 μm (Yan *et al.*, 2013). The custom-made rod stimulator was

556   composed of a miniature loudspeaker (LSM-S20K, EKULIT), to which a blunt metal rod was adhered.

557   The loudspeaker was connected to an electric pulse generator (SD9 Stimulator, Grass Products,

558   Warwick, Rhode Island, U.S.A.). By generating rectangular impulses, the diaphragm of the loudspeaker

559   was vibrating and hence the metal rod was displaced. Intensity and duration of the impulse were

560   regulated by the stimulator settings. The metal rod was positioned laterally to the animal's body wall

561   touching only one body hemisegment. A gentle mechanical touch (deflection of < 40 μm) (Yan *et al.*,

562   2013) was provoked at 100 Volt with a duration of 100ms. Each stimulation consisted of 5 body wall

563   touches at 5Hz. The pulse generator was externally triggered by imaging software.

564   For pharmacological stimulation of the VUM neuron system we applied 5 µl of Pilocarpine (10^{-4}

565   molar; 0,0244mg/ml) onto the *in vivo* brain dissection. Pilocarpine, a muscarinic agonist which mimics

566   the action of neurotransmitter acetylcholine by binding muscarinic acetylcholine receptors is not

567   hydrolyzed by the acetylcholinesterase.

568

569   ***Functional in vivo calcium (Ca^{2+}) imaging.*** We used an upright fluorescence microscope, Axioskop FS

570   (Zeiss, Germany), equipped with a 10x (UMPlanFL 10x/0.30 w), 20x (XLUMPlanFL 20x/0.95 w) and 40x

571   (LUMPlanFl 40x/0.80 w) water immersion Olympus objective. A Polychrome II (xenon-lamp, 75 W,

572   Photonics, Planegg/Germany), provided light excitation at 475 nm and a filter set (Omega Optical,

573   Vermont, USA) ensured passage of only relevant wavelengths (dichromatic mirror: DCLP500, emission

574   filter: LP515). The emitted light was captured by a 12 bit CCD camera (SensiCam QE, pco.imaging,

575   Germany) with a symmetrical binning of 4 (1.25x1.25 µm/pixel). For imaging measurements, a series

576   of either 300 or 600 images (henceforth frames; 344x260 pixel) was recorded at 5 or 2 Hz, respectively.

577   Longtime and low frequency measurements were used for observations without stimulations whereas

578   short time and high frequency measurements were used for multiple stimulation trials. When

579   stimulated, three successive stimulations with an inter stimulus interval (ISI) of 20 seconds were

580   applied at 10, 30 and 50 seconds into the recording (frame 50, 150 and 250, respectively). All imaging

581   data were analyzed using custom written software in IDL (Interactive Data Language, ITT Visual

582   Information Solutions). A bleaching correction was applied for each frame by subtracting the median

583   fluorescence from each pixel. An automated movement correction compensated for movement

584   artifacts occurring during image sequence recordings. For data acquisition, we set regions of interest

585   (ROIs) for each identifiable VUM neuron cell body cluster in the ventral nerve cord (VNC) of each

586   animal. Mean values of each ROI (5x5 pixels per cluster) were calculated in each image (frame) of the

587   recorded sequence. A data matrix was generated for the fluorescence changes of each identified

588   cluster over all images (frames) recorded in one sequence. To achieve a comparable standard for the

589   calculation of the relative fluorescence changes we first calculated the $\Delta F/F_0$ and defined the

590   background fluorescence (F_0) as the mean of 10 successive frames at the beginning of each recording

591   (frame 5 - 15). Second, we calculated relative values for $\Delta F/F_0$ in percent (%) which are plotted in the

592   figures. For isolated brain imaging experiments each cluster response was normalized to its own

593   strongest response, meaning that each cluster had a 100% value. Only fluorescence values of cluster

594   crossing the half maximum threshold (50%) were taken into account for the wave pattern analysis. For

595   *in vivo* imaging experiments cluster responses were normalized within each animal to its strongest

596   response (100%) over all identified cluster, meaning that only one cluster had a 100% value.

597   Normalized responses of VUM neuron cell body clusters were compared between test groups using

598   unpaired t-tests with Welch's correction for unequal variance when needed using statistical software

599   (Prism, GraphPad Software, La Jolla, California, USA).

600

601   ***Behavioral experiments.*** The foraging behavior of 3rd instar larvae was investigated in glass dishes

602   (13.5 cm Ø) which were cast using standard agarose (Axon Labortechnik, Kaiserslautern, Germany) in

603   bidistilled water (2 mg/100 ml). The crawling events during normal foraging behavior and stimulus

604   induced escape response of the animals were counted and their frequencies analyzed. Observations

605   and mechanical stimulations were done at 26-27°C. For brush or rod stimulations either a handhold

606   brush or a handhold rod stimulator (triggered by hand at the pulse generator) was used to stimulate

607   the posterior end of the larvae. Quiescent animals or animals showing freezing or rolling behavior after

608   mechanical stimulations were excluded from the analysis. Each experimental run started with the

609   observation of the unstimulated foraging behavior during 20 seconds followed by the first stimulation.

610   In total three successive stimulations with an ISI of 20 seconds were applied at 20, 40 and 60 seconds

611   into the experimental run. After each stimulation the crawling events during 20 seconds were counted.

612   For comparisons between different experimental groups a crawling index was calculated by dividing

613   the number of crawling events after each stimulation through the number of crawling events of

614   unstimulated animals before the first stimulation,

615
$$\textbf{crawling index (CI)} = \frac{\textbf{crawling frequency after stimulation i}}{\textbf{crawling frequency before stimulation}}.$$

616   For correlation analysis between calcium imaging measurements and the behavioral performances we

617   did linear regression analysis and calculated Pearson's correlation coefficients (Fig. 4B).

618

619   ***Immunohistochemical staining and confocal imaging.*** To visualize peripheral VUM neuron projections

620   and innervation of body wall muscles in relation to neuronal muscular junctions (Fig. 4A) 3rd instar

621   larvae of Tdc2-GAL4/UAS-GCaMP3.0 flies were pinned on Sylgard dishes as described above. All organs

622   were removed, and the body wall was fixed at six points using Minutien pins. The tissue was fixed for

623   10 minutes in 4% PFA (diluted in 0.1 M PBS), rinsed and washed several times in 0.1 M PBS-0.3% Triton

624   X (PBS-Tx) and blocked 30 minutes in 10% normal goat serum (NGS, diluted in PBS-Tx). The blocking

625   solution was exchanged with antiserum solution: rabbit-anti-GFP (Abcam 290, 1:1000) and mouse-

626   anti-highwire (DSHB #6H4, 1:100) in 10% NGS. Tissue was incubated overnight at 4°C, washed 3 x 10

627   minutes in PBS-Tx and incubated for 2 hours (at room temperature) in second antiserum solution:

628   goat-anti-rabbit-Alexa 488 (Invitrogen A-11008), goat-anti-mouse-Alexa 647 (Invitrogen A-21236) and

629   Phalloidin-Alexa 594 (Invitrogen A12381). Tissue was washed in PBS and mounted in Vectashield (H-

630   1000, Burlingame, Ca). To analyze central thoracic and abdominal VUM clusters (Suppl. Fig. 2A) larval

631   brains (Tdc2-GAL4/UAS-GCaMP3.0) were dissected, fixed, washed and mounted in vectashield.

632   Samples were stored at 4°C until being imaged with a Leica DMi8 CEL SP8 confocal microscope, 8-bit,

633   0.3 mm voxel depth (1.024 x 1.024 px). A 63x/1.40 HC PL APO Oil CS2 WD 0.14 mm objective was used.

634   Images were processed with the freeware imaging software FIJI (Schindelin *et al.*, 2012) and the Leica

635   Application Suite (LAS) X 3D analysis software.

636

Author contributions

638   H.-J.P. and M.S. planned and designed the experiments. M.S., F.B. and M.-M.G. conducted functional

639   calcium imaging experiments. A.S. performed confocal imaging. M.S., F.B. and M.-M.G. analyzed the

640   data. H.-J.P. and M.S. drafted the manuscript.

641

Acknowledgments

648

References

650

651   Arikawa, K., Washio, H. & Tanaka, Y. (1984) Dorsal unpaired median neurons of the cockroach
652   metathoracic ganglion. *J Neurobiol*, **15**, 531-536.

653
654   Baier, A., Wittek, B. & Brembs, B. (2002) Drosophila as a new model organism for the neurobiology of
655   aggression? *J Exp Biol*, **205**, 1233-1240.

656
657   Bässler, U. (1986) On the definition of central pattern generator and its sensory control. *Biological
658   Cybernetics*, **54**, 65-69.

659
660   Baudoux, S. & Burrows, M. (1998) Synaptic activation of efferent neuromodulatory neurones in the
661   locust Schistocerca gregaria. *J Exp Biol*, **201**, 3339-3354.

662
663   Baudoux, S., Duch, C. & Morris, O.T. (1998) *Coupling of Efferent Neuromodulatory Neurons to
664   Rhythmical Leg Motor Activity in the Locust*.

665
666   Berni, J., Pulver, S.R., Griffith, L.C. & Bate, M. (2012) Autonomous circuitry for substrate exploration in
667   freely moving Drosophila larvae. *Curr Biol*, **22**, 1861-1870.

668

669   Bräunig, P. & Pflüger, H.-J. (2001) The unpaired median neurons of insects *Advances in Insect*
670   *Physiology*. Academic Press, pp. 185-IN182.

672   Brembs, B., Christiansen, F., Pfluger, H.J. & Duch, C. (2007) Flight initiation and maintenance deficits in
673   flies with genetically altered biogenic amine levels. *Journal of Neuroscience*, **27**, 11122-11131.

675   Burrows, M. & Pflüger, H.J. (1995) Action of locust neuromodulatory neurons is coupled to specific
676   motor patterns. *J Neurophysiol*, **74**, 347-357.

678   Busch, S., Selcho, M., Ito, K. & Tanimoto, H. (2009) A Map of Octopaminergic Neurons in the Drosophila
679   Brain. *Journal of Comparative Neurology*, **513**, 643-667.

681   Busch, S. & Tanimoto, H. (2010) Cellular configuration of single octopamine neurons in Drosophila.
682   *Journal of Comparative Neurology*, **518**, 2355-2364.

684   Büschges, A., Schmitz, J. & Bassler, U. (1995) Rhythmic Patterns in the Thoracic Nerve Cord of the Stick
685   Insect Induced by Pilocarpine. *Journal of Experimental Biology*, **198**, 435-456.

687   Candy, D.J. (1978) Regulation of Locust Flight-Muscle Metabolism by Octopamine and Other
688   Compounds. *Insect Biochem*, **8**, 177-181.

690   Chentsova, N.A., Gruntenko, N.E., Bogomolova, E.V., Adonyeva, N.V., Karpova, E.K. & Rauschenbach,
691   I.Y. (2002) Stress response in Drosophila melanogaster strain inactive with decreased tyramine
692   and octopamine contents. *J Comp Physiol B*, **172**, 643-650.

694   Crisp, S., Evers, J.F., Fiala, A. & Bate, M. (2008) The development of motor coordination in Drosophila
695   embryos. *Development*, **135**, 3707-3717.

697   Crossman, A.R., Kerkut, G.A. & Walker, R.J. (1971) Axon pathways of electrically excitable nerve cell
698   bodies in the insect central nervous system. *J Physiol*, **218 Suppl**, 55P-56P.

700   Dixit, R., Vijayraghavan, K. & Bate, M. (2008) Hox genes and the regulation of movement in Drosophila.
701   *Dev Neurobiol*, **68**, 309-316.

703   Duch, C., Mentel, T. & Pfluger, H.J. (1999) Distribution and activation of different types of
704   octopaminergic DUM neurons in the locust. *J Comp Neurol*, **403**, 119-134.

706   Duch, C. & Pflüger, H.J. (1999) DUM neurons in locust flight: a model system for amine-mediated
707   peripheral adjustments to the requirements of a central motor program. *J Comp Physiol A*,
708   **184**, 489-499.

710   El-Kholy, S., Stephano, F., Li, Y., Bhandari, A., Fink, C. & Roeder, T. (2015) Expression analysis of
711   octopamine and tyramine receptors in Drosophila. *Cell Tissue Res*, 1-16.

712

713   Erspamer, V. (1948) Active Substances in the Posterior Salivary Glands of Octopoda .2. Tyramine and
714   Octopamine (Oxyoctopamine). *Acta Pharmacol Tox*, **4**, 224-247.

715
716   Farooqui, T. (2012) Review of octopamine in insect nervous systems. *Open Access Insect Physiol*, **4**, 1-
717   17.

718
719   Fox, L.E., Soll, D.R. & Wu, C.F. (2006) Coordination and modulation of locomotion pattern generators
720   in Drosophila larvae: effects of altered biogenic amine levels by the tyramine beta hydroxlyase
721   mutation. *J Neurosci*, **26**, 1486-1498.

722
723   Fussnecker, B.L., Smith, B.H. & Mustard, J.A. (2006) Octopamine and tyramine influence the behavioral
724   profile of locomotor activity in the honey bee (Apis mellifera). *J Insect Physiol*, **52**, 1083-1092.

725
726   Gomez-Marin, A. & Louis, M. (2012) Active sensation during orientation behavior in the Drosophila
727   larva: more sense than luck. *Curr Opin Neurobiol*, **22**, 208-215.

728
729   Green, C.H., Burnet, B. & Connolly, K.J. (1983) Organization and patterns of inter- and intraspecific
730   variation in the behaviour of Drosophila larvae. *Animal Behaviour*, **31**, 282-291.

731
732   Hammer, M. (1993) An identified neuron mediates the unconditioned stimulus in associative olfactory
733   learning in honeybees. *Nature*, **366**, 59-63.

734
735   Hammer, M. & Menzel, R. (1998) Multiple sites of associative odor learning as revealed by local brain
736   microinjections of octopamine in honeybees. *Learn Mem*, **5**, 146-156.

737
738   Heckscher, E.S., Lockery, S.R. & Doe, C.Q. (2012) Characterization of Drosophila larval crawling at the
739   level of organism, segment, and somatic body wall musculature. *J Neurosci*, **32**, 12460-12471.

740
741   Hirashima, A., Sukhanova, M. & Rauschenbach, I. (2000) Genetic control of biogenic-amine systems in
742   Drosophila under normal and stress conditions. *Biochem Genet*, **38**, 167-180.

743
744   Hoyer, S.C., Eckart, A., Herrel, A., Zars, T., Fischer, S.A., Hardie, S.L. & Heisenberg, M. (2008)
745   Octopamine in male aggression of Drosophila. *Curr Biol*, **18**, 159-167.

746
747   Hoyle, G. (1974) Function for Neurons (Dum) Neurosecretory on Skeletal-Muscle of Insects. *J Exp Zool*,
748   **189**, 401-406.

749
750   Hoyle, G. (1975) Evidence that insect dorsal unpaired median (DUM) neurons are octopaminergic. *J
751   Exp Zool*, **193**, 425-431.

752
753   Hoyle, G. & Dagan, D. (1978) Physiological Characteristics and Reflex Activation of Dum
754   (Octopaminergic) Neurons of Locust Metathoracic Ganglion. *J Neurobiol*, **9**, 59-79.

755

756   Hu, C., Petersen, M., Hoyer, N., Spitzweck, B., Tenedini, F., Wang, D., Gruschka, A., Burchardt, L.S.,
757   Szpotowicz, E., Schweizer, M., Guntur, A.R., Yang, C.H. & Soba, P. (2017) Sensory integration
758   and neuromodulatory feedback facilitate Drosophila mechanonociceptive behavior. *Nat*
759   *Neurosci*, **20**, 1085-1095.

760

761   Ji, R.-R., Kohno, T., Moore, K.A. & Woolf, C.J. (2003) Central sensitization and LTP: do pain and memory
762   share similar mechanisms? *Trends in Neurosciences*, **26**, 696-705.

763

764   Johnston, R.M., Consoulas, C., Pfl ger, H. & Levine, R.B. (1999) Patterned activation of unpaired median
765   neurons during fictive crawling in manduca sexta larvae. *J Exp Biol*, **202 (Pt 2)**, 103-113.

766

767   Johnston, R.M. & Levine, R.B. (1996) Crawling motor patterns induced by pilocarpine in isolated larval
768   nerve cords of Manduca sexta. *J Neurophysiol*, **76**, 3178-3195.

769

770   Kononenko, N.L. & Pflüger, H.J. (2007) Dendritic projections of different types of octopaminergic
771   unpaired median neurons in the locust metathoracic ganglion. *Cell Tissue Res*, **330**, 179-195.

772

773   Koon, A.C., Ashley, J., Barria, R., DasGupta, S., Brain, R., Waddell, S., Alkema, M.J. & Budnik, V. (2011)
774   Autoregulatory and paracrine control of synaptic and behavioral plasticity by octopaminergic
775   signaling. *Nat Neurosci*, **14**, 190-199.

776

777   Koon, A.C. & Budnik, V. (2012) Inhibitory control of synaptic and behavioral plasticity by
778   octopaminergic signaling. *J Neurosci*, **32**, 6312-6322.

779

780   Lahiri, S., Shen, K., Klein, M., Tang, A., Kane, E., Gershow, M., Garrity, P. & Samuel, A.D. (2011) Two
781   alternating motor programs drive navigation in Drosophila larva. *PLoS One*, **6**, e23180.

782

783   Mentel, T., Duch, C., Stypa, H., Wegener, G., Muller, U. & Pfluger, H.-J. (2003) Central modulatory
784   neurons control fuel selection in flight muscle of migratory locust. *The Journal of neuroscience*
785   *: the official journal of the Society for Neuroscience*, **23**, 1109-1113.

786

787   Mentel, T., Weiler, V., Buschges, A. & Pfluger, H.J. (2008) Activity of neuromodulatory neurones during
788   stepping of a single insect leg. *J Insect Physiol*, **54**, 51-61.

789

790   Monastirioti, M. (1999) Biogenic amine systems in the fruit fly Drosophila melanogaster. *Microsc Res*
791   *Tech*, **45**, 106-121.

792

793   Monastirioti, M., Gorczyca, M., Rapus, J., Eckert, M., White, K. & Budnik, V. (1995) Octopamine
794   immunoreactivity in the fruit fly Drosophila melanogaster. *J Comp Neurol*, **356**, 275-287.

795

796   Orchard, I. & Lange, A.B. (1986) Neuromuscular-Transmission in an Insect Visceral Muscle. *J Neurobiol*,
797   **17**, 359-372.

798

799   Ormerod, K.G., Hadden, J.K., Deady, L.D., Mercier, A.J. & Krans, J.L. (2013) *Action of octopamine and*
800   *tyramine on muscles of Drosophila melanogaster larvae.*

801

802   Ormerod, K.G., Jung, J. & Mercier, A.J. (2018) Modulation of neuromuscular synapses and contraction
803   in Drosophila 3rd instar larvae. *J Neurogenet*, **32**, 183-194.

804

805   Papaefthmiou, C. & Theophilidis, G. (2001) An in vitro method for recording the electrical activity of
806   the isolated heart of the adult Drosophila melanogaster. *In Vitro Cell Dev Biol Anim*, **37**, 445-
807   449.

808

809   Pauls, D., Blechschmidt, C., Frantzmann, F., el Jundi, B. & Selcho, M. (2018) A comprehensive
810   anatomical map of the peripheral octopaminergic/tyraminergic system of Drosophila
811   melanogaster. *Scientific Reports*, **8**, 15314.

812

813   Pflüger, H.J. & Duch, C. (2011) Dynamic neural control of insect muscle metabolism related to motor
814   behavior. *Physiology (Bethesda)*, **26**, 293-303.

815

816   Plotnikova, S. (1969) Effector neurons with several axons in the ventral nerve cord of the Asian
817   grasshopper Locusta migratoria. *J Evol Biochem Physiol*, **5**, 276-277.

818

819   Pulver, S.R., Bayley, T.G., Taylor, A.L., Berni, J., Bate, M. & Hedwig, B. (2015) Imaging fictive locomotor
820   patterns in larval Drosophila. *J Neurophysiol*, **114**, 2564-2577.

821

822   Roeder, T. (2005) Tyramine and octopamine: ruling behavior and metabolism. *Annu Rev Entomol*, **50**,
823   447-477.

824

825   Roeder, T., Seifert, M., Kahler, C. & Gewecke, M. (2003) Tyramine and octopamine: antagonistic
826   modulators of behavior and metabolism. *Arch Insect Biochem Physiol*, **54**, 1-13.

827

828   Ryckebusch, S. & Laurent, G. (1993) Rhythmic patterns evoked in locust leg motor neurons by the
829   muscarinic agonist pilocarpine. *J Neurophysiol*, **69**, 1583-1595.

830

831   Saraswati, S., Fox, L.E., Soll, D.R. & Wu, C.F. (2004) Tyramine and octopamine have opposite effects on
832   the locomotion of Drosophila larvae. *J Neurobiol*, **58**, 425-441.

833

834   Scheiner, R., Baumann, A. & Blenau, W. (2006) Aminergic control and modulation of honeybee
835   behaviour. *Curr Neuropharmacol*, **4**, 259-276.

836

837   Schindelin, J., Arganda-Carreras, I., Frise, E., Kaynig, V., Longair, M., Pietzsch, T., Preibisch, S., Rueden,
838   C., Saalfeld, S., Schmid, B., Tinevez, J.-Y., White, D.J., Hartenstein, V., Eliceiri, K., Tomancak, P.
839   & Cardona, A. (2012) Fiji: an open-source platform for biological-image analysis. *Nature*
840   *Methods*, **9**, 676.

841

842   Schroll, C., Riemensperger, T., Bucher, D., Ehmer, J., Voller, T., Erbguth, K., Gerber, B., Hendel, T., Nagel,
843   G., Buchner, E. & Fiala, A. (2006) Light-induced activation of distinct modulatory neurons
844   triggers appetitive or aversive learning in Drosophila larvae. *Curr Biol*, **16**, 1741-1747.

845

846   Schützler, N., Girwert, C., Hügli, I., Mohana, G., Roignant, J.-Y., Ryglewski, S. & Duch, C. (2019) Tyramine
847   action on motoneuron excitability and adaptable tyramine/octopamine ratios adjust
848   Drosophila locomotion to nutritional state. *Proceedings of the National Academy of Sciences*,
849   **116**, 3805-3810.

850

851   Selcho, M., Pauls, D., El Jundi, B., Stocker, R.F. & Thum, A.S. (2012) The role of octopamine and tyramine
852   in Drosophila larval locomotion. *J Comp Neurol*, **520**, 3764-3785.

853

854   Selcho, M., Pauls, D., Huser, A., Stocker, R.F. & Thum, A.S. (2014) Characterization of the
855   octopaminergic and tyraminergic neurons in the central brain of Drosophila larvae. *J Comp*
856   *Neurol*, **522**, 3485-3500.

857

858   Sombati, S. & Hoyle, G. (1984) Generation of specific behaviors in a locust by local release into neuropil
859   of the natural neuromodulator octopamine. *J Neurobiol*, **15**, 481-506.

860

861   Song, W., Onishi, M., Jan, L.Y. & Jan, Y.N. (2007) Peripheral multidendritic sensory neurons are
862   necessary for rhythmic locomotion behavior in Drosophila larvae. *Proc Natl Acad Sci U S A*,
863   **104**, 5199-5204.

864

865   Stevenson, P.A., Dyakonova, V., Rillich, J. & Schildberger, K. (2005) Octopamine and experience-
866   dependent modulation of aggression in crickets. *J Neurosci*, **25**, 1431-1441.

867

868   Stolz, T., Diesner, M., Neupert, S., Hess, M.E., Delgado-Betancourt, E., Pflüger, H.-J. & Schmidt, J. (2019)
869   Descending octopaminergic neurons modulate sensory-evoked activity of thoracic motor
870   neurons in stick insects. *Journal of Neurophysiology*, **122**, 2388-2413.

871

872   Sujkowski, A., Ramesh, D., Brockmann, A. & Wessells, R. (2017) Octopamine Drives Endurance Exercise
873   Adaptations in Drosophila. *Cell Rep*, **21**, 1809-1823.

874

875   Suo, S., Culotti, J.G. & Van Tol, H.H. (2009) Dopamine counteracts octopamine signalling in a neural
876   circuit mediating food response in C. elegans. *EMBO J*, **28**, 2437-2448.

877

878   Tabuena, D.R., Solis, A., Geraldi, K., Moffatt, C.A. & Fuse, M. (2017) Central neural alterations
879   predominate in an insect model of nociceptive sensitization. *Journal of Comparative*
880   *Neurology*, **525**, 1176-1191.

881

882   Tian, L., Hires, S.A., Mao, T., Huber, D., Chiappe, M.E., Chalasani, S.H., Petreanu, L., Akerboom, J.,
883   McKinney, S.A., Schreiter, E.R., Bargmann, C.I., Jayaraman, V., Svoboda, K. & Looger, L.L. (2009)
884   Imaging neural activity in worms, flies and mice with improved GCaMP calcium indicators. *Nat*
885   *Methods*, **6**, 875-881.

886

887   Vömel, M. & Wegener, C. (2008) Neuroarchitecture of aminergic systems in the larval ventral ganglion
888   of Drosophila melanogaster. *PLoS One*, **3**, e1848.

889

890   Waddell, S. (2013) Reinforcement signalling in Drosophila; dopamine does it all after all. *Curr Opin*
891   *Neurobiol*, **23**, 324-329.

892

893   Walters, E., Illich, P., Weeks, J. & Lewin, M. (2001) Defensive responses of larval Manduca sexta and
894   their sensitization by noxious stimuli in the laboratory and field. *Journal of Experimental*
895   *Biology*, **204**, 457-469.

896

897   Walther, C. & Zittlau, K.E. (1998) Resting membrane properties of locust muscle and their modulation
898   II. Actions of the biogenic amine octopamine. *J Neurophysiol*, **80**, 785-797.

899

900   Watson, A.H. (1984) The dorsal unpaired median neurons of the locust metathoracic ganglion:
901   neuronal structure and diversity, and synapse distribution. *J Neurocytol*, **13**, 303-327.

902

903   Wicher, D. (2007) Metabolic regulation and behavior: how hunger produces arousal - an insect study.
904   *Endocr Metab Immune Disord Drug Targets*, **7**, 304-310.

905

906   Xiang, Y., Yuan, Q., Vogt, N., Looger, L.L., Jan, L.Y. & Jan, Y.N. (2010) Light-avoidance-mediating
907   photoreceptors tile the Drosophila larval body wall. *Nature*, **468**, 921-926.

908

909   Yan, Z., Zhang, W., He, Y., Gorczyca, D., Xiang, Y., Cheng, L.E., Meltzer, S., Jan, L.Y. & Jan, Y.N. (2013)
910   Drosophila NOMPC is a mechanotransduction channel subunit for gentle-touch sensation.
911   *Nature*, **493**, 221-225.

912

913   Zeng, H., Loughton, B.G. & Jennings, K.R. (1996) Tissue specific transduction systems for octopamine
914   in the locust (Locusta migratoria). *J Insect Physiol*, **42**, 765-769.

915

916   Zhou, C., Rao, Y. & Rao, Y. (2008) A subset of octopaminergic neurons are important for Drosophila
917   aggression. *Nature Neuroscience*, **11**, 1059-1067.

918

919

920